Inorganica Chimica Acta 495 (2019) 118954

Contents lists available at ScienceDirect

Inorganica Chimica Acta

journal homepage: www.elsevier.com/locate/ica

Research paper

Synthesis and characterization of the *trans*(O_6) isomer Ni(II) complex containing symmetrical edta-type ligand with mixed carboxylate and diamine rings: Quantum-mechanical evaluation of different isomers

Marija S. Jeremić[a], Marko D. Radovanović[a], Olivera R. Klisurić[b], Svetlana K. Belošević[c], Zoran D. Matović[a,*]

[a] University of Kragujevac, Faculty of Science, Department of Chemistry, Radoja Domanovića 12, 34000 Kragujevac, Serbia
[b] University of Novi Sad, Faculty of Sciences, Department of Physics, Trg Dositeja Obradovića 4, 21000 Novi Sad, Serbia
[c] University of Priština, Faculty of Technical Sciences, Knjaza Miloša 7, Kosovska Mitrovica, Serbia

ARTICLE INFO

Keywords:
Nickel(II) chelates
Polyaminopolycarboxylates
X-ray
DFT
NBO

ABSTRACT

The *trans*(O_6) isomer (*trans*(O_6) refer to two six-membered rings in *trans* position) of the $[Ba(H_2O)_4][Ni(1,3\text{-pddadp})]\cdot 4H_2O$ (1,3-pddadp = 1,3-propanediamine-*N,N′*-diacetate-*N,N′*-di-3-propionate) was synthesized and spectroscopically characterized (IR, UV–Vis). The *trans*(O_6) geometry was confirmed by X-ray diffraction analysis. Single crystal X-ray diffraction of the complex revealed an octahedral geometry around the Ni(II) centre. Extensive strain analysis of $[M(\text{edta-type})]^{2-}$ complexes (M = Ni, Co, Cu) has been performed and discussed in detail. DFT/NBO analysis (DFT = Density Functional Theory, NBO = Natural Bond Orbital) was performed for all isomers of $[Ni(1,3\text{-pddadp})]^{2-}$ complex. DFT theory shows that *trans*(O_6) isomer is 0.53 kcal mol^{-1} more stable than *trans*(O_5O_6) and 1.95 kcal mol^{-1} more stable than *trans*(O_5). NBO analysis for all three isomers predicts the existence of a 3-center 2-electron (β system) A: -Ni-: B hyperbonds along with O:-C-:O carboxylate triads. The Second-Order Perturbation Theory Analysis predicts molecular stabilization that comes from delocalization caused by $n_A \rightarrow \sigma_{NiB^*}$ or $n_B \rightarrow \sigma_{NiA^*}$ charge transfer.

1. Introduction

The eddadp (ethylenediamine-*N,N′*-diacetate-*N,N′*-di-3-propionate) and 1,3-pddadp (1,3-propanediamine-*N,N′*-diacetate-*N,N′*-di-3-propionate), belong to the group of edta-type of ligands (edta = ethylenediamine-*N,N,N′,N′*-tetraacetate). These ligands upon full coordination to the central metal ion form three geometrical isomers (Fig. 1): *trans*(O_5), *trans*(O_5O_6) and *trans*(O_6) (O_5 and O_6 relate to the five- and six-membered carboxylate ring respectively). It has been shown that the six-membered propionate rings serve better for the formation of the less-strained in-plane G rings favoring the *trans*(O_5) isomers of $[M(\text{eddadp})]^{n-}$ (M = Cr(III), Fe(III), Co(III), Rh(III), Co(II), Ni(II), Cu(II)) complexes, with 6-5-6 in-plane arrangement of rings [1–10]. After reviewing the synthesized $[M(1,3\text{-pddadp})]^{n-}$ complexes, one can observe the following layout of the isomers prepared: all three possible isomers have been reported for Cr(III) (3D structure was X-ray portrayed for the *trans*(O_6) isomer [11]); only *trans*(O_6) isomer has been prepared and X-ray determined for Cu(II) [12]; for Co(III) the *trans*(O_5O_6) and *trans*(O_6) isomers were isolated [13,14] but the *trans*(O_5) and *trans*(O_5O_6) in case of Rh(III) [15]. Similarly to Rh(III), the *trans*(O_5) and *trans*(O_5O_6) isomers of nickel(II) have been prepared and isolated. The 3D structure was confirmed by X-ray for *trans*(O_5) isomer. The *trans*(O_6) isomer has not been even detected under chromatographic conditions [16].

Molecular structures of edta and related transition-metal complexes have been discussed in terms of the *d*-electron configuration, size of the central metal ion (M) and the structure of the ligand. These influence the differences in the bond lengths (M—N and M—O), ring strain and the ligand configuration [3–11,14–27]. The significance of the ligand strain becomes important when it comes to the deviation of the bonding angles from the ideal values in $[M(\text{edta})]^{n-}$ (M = Co(III) [17], Co(II) [18], Ni(II) [19–21]) and other edta-metal complexes. In these complexes a much higher strain of the acetate rings (G rings) and one ethylenediamine ring (E ring) contained in-plane with respect to the acetate rings in an axial position was observed.

In this paper, we have prepared and characterized the missing *trans*(O_6) isomer of $[Ni(II)(1,3\text{-pddadp})]^{2-}$ complex. Its 3D structure has been confirmed by X-ray analysis. DFT (Density Functional Theory) methods

* Corresponding author.
E-mail address: zmatovic@kg.ac.rs (Z.D. Matović).

https://doi.org/10.1016/j.ica.2019.118954
Received 13 April 2019; Received in revised form 5 June 2019; Accepted 5 June 2019
Available online 06 June 2019
0020-1693/

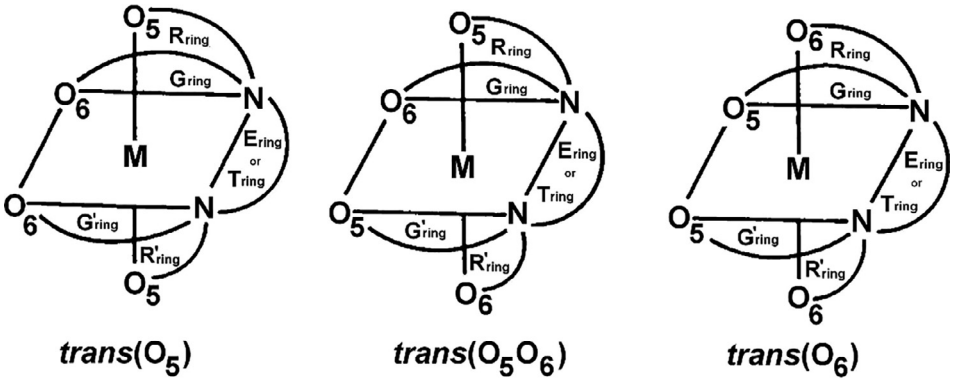

Fig. 1. Three possible geometrical isomers of hexadentate $[M(eddadp)]^{n-}$ and $[M(1,3\text{-}pddadp)]^{n-}$ complexes (E = the five-membered ethylenediamine ring; T = the six-membered 1,3-propanediamine ring, R = the five- or six-membered carboxylate ring in axial position, G = the five- or six-membered carboxylate ring in-plane).

Table 1
Crystal data and structure refinement for *trans*(O_6)-[$Ba(H_2O)_4$][Ni(1,3-pddadp)]·$4H_2O$ (**1**).

Chemical formula	$C_{13}H_{34}BaN_2NiO_{16}$
M_r	670.47
Crystal system, space group	Triclinic, $P-1$
a, *b*, *c* (Å)	9.1850 (6), 12.0034 (8), 12.2326 (7)
α, β, γ(°)	101.841 (5), 109.551 (6), 95.576 (6)
V (Å^3)	1223.58 (14)
Z	2
F(0 0 0)	676
D_x (Mg m^{-3})	1.820
No. of reflections for cell measurement	4911
θrange (°) for cell measurement	3.8–72.6
μ (mm^{-1})	14.08
Crystal shape	Prism
Colour	Blue
Crystal size (mm)	0.37 × 0.32 × 0.19
Absorption correction	Gaussian
T_{min}, T_{max}	0.057, 0.256
Reflections collected	7741
Independent reflections	4461
Observed reflections [$I > 2\sigma(I)$]	4226
R_{int}	0.025
$(\sin\theta/\lambda)_{max}$ (Å^{-1})	0.602
θvalues (°)	$\theta_{max} = 68.2$, $\theta_{min} = 4.0$
Range of *h*, *k*, *l*	$h = -11 \rightarrow 5$, $k = -14 \rightarrow 14$, $l = -14 \rightarrow 14$
R, w*R* [$I > 2\sigma(I)$]	0.0256, 0.0647
R, w*R [all data]*	0.0274, 0.0657
Goodness-of-fit on F^2	1.047
No. of reflections	4461
No. of parameters	346
No. of restraints	17
H-atom treatment	H atoms treated by a mixture of independent and constrained refinement
Weighting scheme	$w = 1/[\sigma^2(F_o^2) + (0.0362P)^2 + 0.1649P]$ where $P = (F_o^2 + 2F_c^2)/3$
ρ_{max}, ρ_{min} (e Å^{-3})	0.39, −0.63

have been used for the purpose of energetic analysis and structural comparison [28]. Natural Bonding Orbitals (NBO) analysis [29] have been done for all isomers in question. We tried to compare principal Donor/Acceptor energies against geometric isomerism so make it usable in terms of energetic stability as well as their probability of formation in the solution. Therefore, the aim of this paper is to prepare *trans*(O_6) isomer of $[Ni(II)(1,3\text{-}pddadp)]^{2-}$ complex and isolate it in a crystal form suitable for an X-ray analysis in order to evaluate its structural parameters. This means that we would be able with more confidence to discuss the structure and energetic dependence of all possible geometries. Also, structural parameters and strain analysis data of this and similar complexes of known structures are discussed in relation to the structure of the ligand, geometry of complexes, octahedral distortion and their mutual energetic dependence.

2. Experimental

2.1. Materials and physical measurements

All chemicals were purchased from Sigma-Aldrich and were used without any further purification. 1,3-propanediamine-*N,N′*-diacetic acid dihydrochloride, $H_2$1,3-pdda·2HCl was prepared using a previously described procedure [30].

Elemental (C, H, N) analysis of the sample was carried out in the Center for Instrumental Analysis, Faculty of Chemistry, Belgrade. IR spectra (in KBr pellets) in the 400–4000 cm^{-1} region were recorded on a Perkin–Elmer FT-IR spectrophotometer Spectrum One. Electronic absorption spectra were obtained using a Perkin–Elmer Lambda 35 spectrophotometer. The melting point was measured by Stuart melting device with accuracy ± 1 °C.

2.2. Preparation of complex

2.2.1. Preparation of condensation mixture containing 1,3-propanediamine-N,N′-diacetic-N′-3-propionic acid, $H_3$1,3-pd2ap and 1,3-propanediamine-N,N′-diacetic-N,N′-di-3-propionic acid, $H_4$1,3-pddadp

The reaction mixture was prepared by the method of Belošević et al. [31] starting from 40 mmol of $H_2$1,3-pdda·2HCl.

2.2.2. Preparation of the trans(O_6)-tetraaquobarium[(1,3-propanediamine-N,N′-diacetate-N,N′-di-3-propionate)nickelate(II)] tetrahydrate, trans(O_6)-[$Ba(H_2O)_4$][Ni(1,3-pddadp)]·$4H_2O$ (1)

The synthesis of the nickel(II) complexes was accomplished by the previously reported procedure [31]. The equivalent amount of $NiCl_2$·$6H_2O$ (40 mmol) has been mixed with the above mixture of acids.

The blue filtrate (from the above mixture) was desalted using G-10 Sephadex column, with distilled water as the eluent. To separate the components of the reaction mixture, a chromatographic column (4 × 40 cm) filled with Dowex 1-X8 (200–400 mesh) anion exchange resin in the Cl^- form was used. First, the column was washed with water in order to separate the neutral *cis*-polar-[Ni(1,3-pdda)(H_2O)$_2$] complex. After elution with 0.1 M NaCl, the two bands appeared on the column; the first band quite broad and the second distinct one. The obtained eluates were reduced to a small volume and then desalted using Sephadex G-10 resin. The light blue eluate of the first band was assigned to the *cis*-polar-$[Ni(1,3\text{-}pd2ap)]^-$ isomer [31]. The second blue eluate presents *trans*(O_5)-Na_2[Ni(1,3-pddadp)] isomer of known structure [16]. The first eluate was reduced to a volume of 2 mL and stored in a desiccator over ethanol. The powder of *cis*-polar-[Ni(1,3-

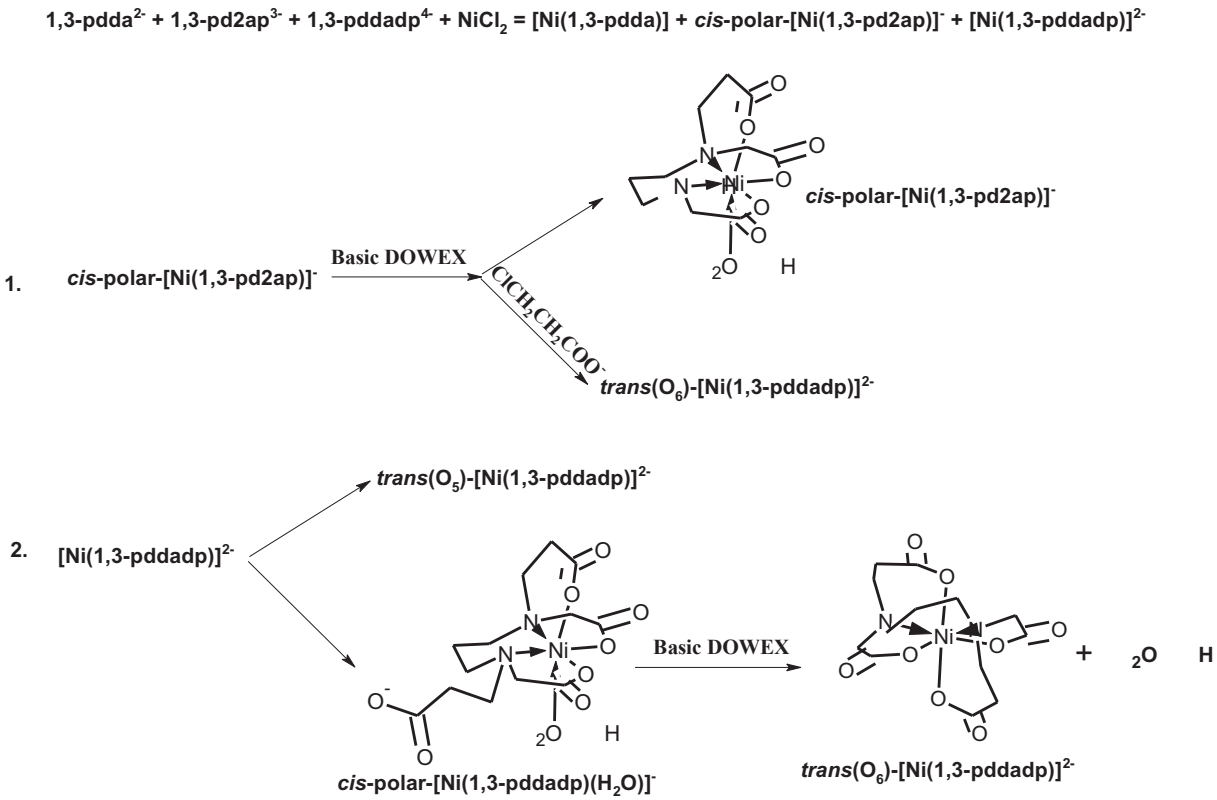

Scheme 1. Schematic route for preparation of *trans*(O_6)-[Ni(1,3-pddadp)]$^{2-}$ ion.

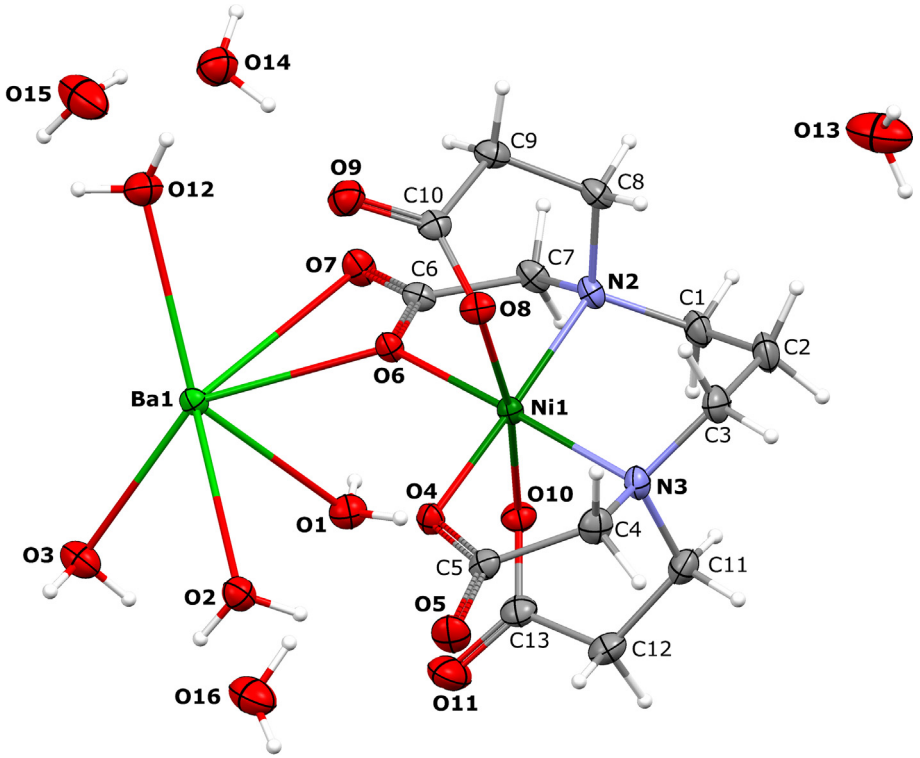

Fig. 2. MERCURY [37] drawing of molecular structure of *trans*(O_6)-[Ba(H_2O)$_4$][Ni(1,3-pddadp)]·4H_2O with the non-H atom numbering scheme (displacement ellipsoids at 30% probability level).

pd2ap)] were removed. The blue filtrate was further evaporated to dryness and reconstituted in 1 mL of water and left to stand in the refrigerator for several weeks. Blue crystals were collected, washed with ethanol and then with ether, and air-dried. Recrystallization was carried out from the water. Blue crystals from the solution represent the complex *trans*(O_6)-Na_2[Ni(1,3-pddadp)]·2.5H_2O Yield: 0.65 g (3.4%). Melting point = 211 °C Anal. Calc. for. $Na_2NiC_{13}H_{23}N_2O_{10.5}$ (Mw = 480.00) C: 32.53, H: 4.83, N: 5.84; found: C: 32.85, H: 4.90, N:

Table 2
Selected geometric parameters for *trans*(O_6)-[$Ba(H_2O)_4$][Ni(1,3-pddadp)]·4H_2O (**1**).

Bond length [Å]			
[Ni(1,3-pddadp)]$^{2-}$		*[Ba(H_2O)$_4$(O_G-carbox.)$_2$]*$^{2+}$	
Ni1—N2	2.083 (3)	Ba1—O1	2.829 (3)
Ni1—N3	2.084 (3)	Ba1—O2	2.926 (2)
Ni1—O4	2.040 (2)	Ba1—O3	2.788 (3)
Ni1—O6	2.038 (2)	Ba1—O12	2.841 (3)
Ni1—O8	2.109 (2)	Ba1—O2^2	2.968 (3)
Ni1vO10	2.129 (2)	Ba1—O4^2	2.877 (2)
		Ba1—O5^2	3.003 (3)
		Ba1—O7^1	2.724 (2)
Bond angles [°]			
[Ni(1,3-pddadp)]$^{2-}$		*[Ba(H_2O)$_4$(O_G-carbox.)$_2$]*$^{2+}$	
O6—Ni1—N2	82.11 (9)	O3—Ba1—O1	77.75 (8)
N2—Ni1—N3	97.07 (10)	O6—Ba1—O1	69.63 (7)
O4—Ni1—N3	82.67 (10)	O6—Ba1—O12	86.39 (7)
O6—Ni1—O8	88.36 (9)	O3—Ba1—O12	128.77 (9)
N2—Ni1—O8	89.19 (10)	O1—Ba1—O12	134.14 (8)
N3—Ni1—O8	97.26 (10)	O6—Ba1—O3	143.77 (8)
O4—Ni1—O8	86.56 (9)	O1—Ba1—O2	70.88 (7)
O4—Ni1—O10	88.45 (9)	O6—Ba1—O2	82.72 (7)
N2—Ni1—O10	95.87 (10)	O3—Ba1—O2	71.85 (8)
N3—Ni1—O10	89.20 (10)	O12—Ba1—O2	145.88 (8)
O6—Ni1—O10	85.30 (9)	O6—Ba1—O7	45.49 (6)
O4—Ni1—N2	175.67 (10)	O3—Ba1—O7	132.41 (7)
O6—Ni1—N3	174.31 (10)	O1—Ba1—O7	67.35 (7)
O8—Ni1—O10	171.27 (9)	O12—Ba1—O7	68.00 (8)

Symmetry codes: [1]: $-x+1, -y, -z+2$; [2]: $-x+2, -y, -z+2$.

Table 3
Hydrogen bond parameters for *trans*(O_6)-[$Ba(H_2O)_4$][Ni(1,3-pddadp)]·4H_2O (**1**).

D—H···*A*	*D*—H (Å)	H···*A* (Å)	*D*···*A* (Å)	*D*—H···*A* (°)
O1—H1C···O10	0.850 (19)	1.96 (2)	2.810 (3)	175 (5)
O1—H1C···O11	0.850 (19)	2.48 (4)	3.056 (4)	126 (4)
O1—H1D···O12^1	0.837 (19)	1.96 (2)	2.779 (4)	167 (5)
O2—H2C···O9^2	0.828 (19)	2.13 (2)	2.948 (4)	170 (5)
O2—H2D···O11	0.845 (19)	2.25 (2)	3.088 (4)	169 (5)
O3—H3C···O16	0.857 (19)	2.09 (2)	2.943 (5)	173 (5)
O3—H3D···O8^2	0.845 (19)	1.98 (2)	2.811 (3)	166 (5)
O3—H3D···O9^2	0.845 (19)	2.53 (4)	3.197 (4)	136 (4)
O12—H12D···O14	0.850 (19)	1.92 (2)	2.757 (4)	169 (5)
O13—H13A···O16^3	0.83 (2)	1.98 (3)	2.783 (6)	160 (5)
O13—H13B···O15^4	0.85 (2)	1.99 (2)	2.819 (5)	164 (5)
O14—H14A···O9	0.851 (19)	1.89 (3)	2.693 (4)	157 (5)
O14—H14B···O13^5	0.840 (19)	1.91 (2)	2.750 (5)	177 (5)
O15—H15A···O14	0.866 (19)	1.92 (2)	2.777 (5)	169 (5)
O16—H16A···O15^2	0.840 (19)	2.19 (2)	3.015 (6)	168 (5)
O16—H16B···O1	0.831 (19)	1.93 (2)	2.743 (4)	165 (5)

Symmetry codes: [1]: $-x+1, -y, -z+2$; [2]: $-x+2, -y, -z+2$; [3]: $x, y+1, z$; [4]: $x-1, y, z-1$; [5]: $-x+1, -y+1, -z+2$.

5.83%.

Complex (**1**) in the form of the barium(II) salt was obtained using the ion-exchange column technique. The eluate was reduced to a small volume and allowed to stand at room temperature to crystallize the complex *trans*(O_6)-[$Ba(H_2O)_4$][Ni(1,3-pddadp)]·4H_2O (**1**). Yield: 0.73 g (2.7%). Melting point = 289 °C; Anal. Calc. for. $BaNiC_{13}H_{34}N_2O_{16}$ (Mw = 670.43) C: 23.29, H: 5.11, N: 4.18; found: C: 23.03, H: 4.94, N: 4.20%. IR (KBr, pellet): ν (cm^{-1}) 1598 ν(COO^-), 1575sh ν(COO^-), 3412 ν(N—H). UV–Vis (H_2O, $C = 10^{-2}$ M): λmax/nm (ε/$L\,mol^{-1}\,cm^{-1}$): 965 (11.4), 1047sh, 769 (2.9), 601 (7.2) and 373 (11.0).

2.3. Crystal structure determination and refinement

The diffraction data for the complex *trans*(O_6)-[$Ba(H_2O)_4$][Ni(1,3-pddadp)]·4H_2O (**1**) were collected at room temperature on Rigaku (Oxford Diffraction) Gemini S diffractometer with a CCD area detector and graphite-monochromated CuK_α radiation (λ = 1.54184 Å) operated at 40 kV and 40 mA. The CrysAlisPro and CrysAlis RED software packages [32] were used for data collection and data integration. The space group determinations were based on an analysis of the Laue class and the systematically absent reflections. Collected data were corrected for absorption effects by using Numerical absorption correction based on Gaussian integration over a multifaceted crystal model [33].

The structures were solved by direct methods using SHELXT [34]. The structures were refined by full-matrix least-squares procedures on F^2 using SHELXL-2014/6 program [34]. All non-hydrogen atoms were refined anisotropically until convergence was reached. The hydrogen atoms linked to the C atoms were placed on calculated positions (C—H = 0.97 Å, with $U_{iso}(H) = 1.2U_{eq}(C)$) and allowed to ride on their carrier atoms. The water molecule hydrogen atoms were located in a difference Fourier map and refined isotropically. All calculations were performed using PLATON [35] implemented in the WINGX [36] system of programs. MERCURY [37] was employed for molecular graphics. The crystal data and refinement parameters are summarized in Table 1.

2.4. Computational details

The geometries for Ni(II) complexes were optimized using Gaussian 09 D01 program [38]. Starting geometries were taken either from experimental X-ray structures or were modeled using molecular mechanics and pre-optimized using semi-empirical method (MOPAC PM6 [39]). For DFT calculations, we used the unrestricted B3LYP hybrid functional [40] and the Ahlrich's TZVP basis set [41]. The Polarizable Continuum Model (PCM) using the integral equation formalism variant (IEFPCM) with water as a solvent has been employed for all complexes [42]. Subsequent frequency calculations at the same level of theory verified that the optimized structures were true local minima on the potential energy surface i.e. there were no imaginary frequencies. For further calculation of intra-molecular orbital interactions, we used NBO6.0 analyses [29].

3. Results and discussion

3.1. Synthesis of trans(O_6)-[$Ba(H_2O)_4$][Ni(1,3-pddadp)]·4H_2O complex

The blue complex *trans*(O_6)-Na_2[Ni(1,3-pddadp)]·2H_2O has been prepared by the reaction of nickel(II) salt with the neutralized edta-type mixture. Barium(II) salt of above complex *trans*(O_6)-[$Ba(H_2O)_4$][Ni(1,3-pddadp)]·4H_2O was obtained using the cation-exchange column technique. Here we must point out that the complex in the synthetic sense was obtained not on purpose because the synthesis was intended for preparation of pentadentate nickel(II) complexes. However, in the successive repetition of the synthesis we realized that after the precipitation of Na[Ni(1,3-pd2ap)] complex, the remaining filtrate shows a slightly different color. After recording the UV–Vis spectrum of the filtrate and the IR spectrum of the solid obtained from the evaporated filtrate, it was evident that we have a complex different from Na[Ni(1,3-pd2ap)] [31] (we refer the readers to the Spectral analysis of Ref. [31] and this paper). It was reasonable then to try fractional crystallization in order to obtain a pure substance, which in this case was successful.

The isomers of the complex $[M(1,3\text{-pddadp})]^{n-}$ were chromatographically separated following the order: *trans*(O_5) (first), *trans*(O_5O_6) (second) and *trans*(O_6) (third) (Fig. 1), as shown in the case of all three isomers of Cr(III) [11], two isomers *trans*(O_5O_6) and *trans*(O_6) in case of Co(III) [13,14] and two isomers *trans*(O_5) and *trans*(O_5O_6) in case of Rh (III) [15] and Ni(II) [16]. To our surprise, our synthesis did not produce

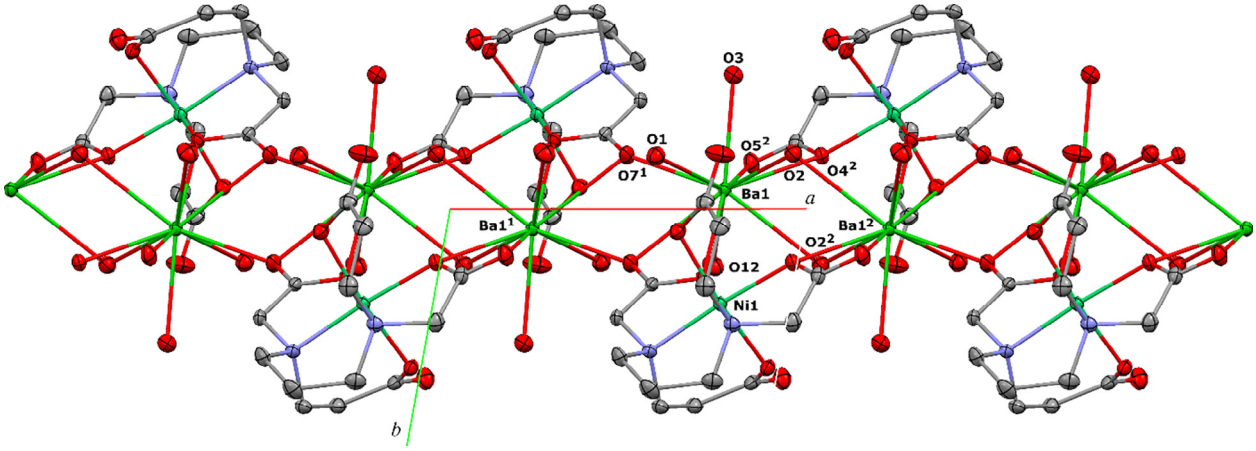

Fig. 3. MERCURY [37] drawing of the crystal packing of *trans*(O_6)-[$Ba(H_2O)_4$][Ni(1,3-pddadp)]·$4H_2O$ showing infinite one-dimensional chains parallel to the *a* axis. Symmetry codes: [1]: $-x+1, -y, -z+2$; [2]: $-x+2, -y, -z+2$. View direction is parallel to the *c* axis. Hydrogen atoms are not shown for clarity.

Table 4
Strain analysis of $[M(edta\text{-}type)]^{2-}$ complexes with five and/or six-membered carboxylate rings.

Complex	$\Sigma\Delta(O_h)$ [a]	$\Delta\Sigma$(ring) [b]			Δ(M−O−C) [c]		$\Sigma\Delta$(N) [d]	Ref.
		E or T	R	G	R	G		
trans(O_5)-[Ni(eddadp)]$^{2-}$	39	−14	0	+39	+7	+20	12	[8]
trans(O_5)-[Ni(1,3-pddadp)]$^{2-}$	60	+28	0	+36	+7	+20	8	[16]
trans(O_5O_6)-[Ni(1,3-pddadp)]$^{2-}$ [e,f]	46	+26	0(+32)	−10(+38)	+8(+18)	+6(+22)	13	This work
trans(O_6)-[Ni(1,3-pddadp)]$^{2-}$	57	+27	+17	−10	+8	+7	12	This work
[Ni(1,3-pdta)]$^{2-}$	60	+33	+1	−11	+6	+6	11	[22]
trans(O_6)-[Co(1,3-pddadp)]$^{2-}$	67	+25	+17	−10	+4	+4	14	[43]
trans(O_6)-[Cu(1,3-pddadp)]$^{2-}$	51	+27	+7	−9	−5	+4	13	[44]

[a] $\Sigma\Delta(O_h)$ is the sum of the absolute values of the deviations from 90° of the twelve L-M-L′ angles. All values rounded off to the nearest degree.
[b] $\Delta\Sigma$(ring) is the deviation from the ideal of the corresponding chelate rings' bond angle sum. Ideal values: 528° for the five-membered ethylenediamine (E) ring, 637.5° for the six-membered 1,3-propanediamine (T) ring, 538.5° and 648° for the five- and six-membered carboxylate (R in axial position and G in-plane) ring, respectively.
[c] Δ(M−O−C) (ring) is the mean value of the deviation of the corresponding rings' M−O−C bond angle from the 109.5°.
[d] $\Sigma\Delta$(N) is the sum of the absolute values of the deviations from 109.5° of the six bond angles made by nitrogen atoms. A mean value for the two nitrogen atoms is reported.
[e] DFT calc. structure (B3LYP/TZVP).
[f] Values in parentheses are given for the 3-propionate rings.

Table 5
Asymmetric carboxylate stretching frequencies for $[Ni(edta\text{-}type)]^-$ complexes.[a]

Complex	ν_{asym} (COOM)	Chelate ring size	Ref.
$[Ni(H_2O)_6]$·[Ni(1,3-pdta)]·$2H_2O$	1587	5	[50]
trans(O_5)-[Ni_2(1,3-pddadp)(H_2O)$_4$]·$4H_2O$	1640sh 1591	5 6	[16]
trans(O_5O_6)-Na_2[Ni(1,3-pddadp)]·$3H_2O$	1635sh 1610 1588	5 6	[16]
trans(O_6)-[$Ba(H_2O)_4$][Ni(1,3-pddadp)]·$4H_2O$	1598 1575sh	5 6	This work

[a] Values are given in cm^{-1}.

trans(O_5) nor *trans*(O_5O_6) isomer while the *trans*(O_6) isomer was isolated by fractional crystallization of the first eluted band. We will try to evaluate these anomalies. First, the reaction mixture, contained edta-type acids, in a quantity order: 1,3-pd2ap > > 1,3-pdda ~ 1,3-pddadp. Such a small quantity of 1,3-pddadp didn't allow the formation of a less favorable *trans*(O_5O_6) isomer in an amount that would be visible on Dowex anion column (Scheme 1). Second, the formation of the *trans*(O_6) isomer could be interpreted in two ways. Both ways appreciate the initial formation of the complex which is the same or similar to *cis*-polar-$[Ni(1,3\text{-}pd2ap)]^-$ isomer [31]. Therefore, it is possible (less likely approach) to imagine an additional reaction of the residual chloro-propionate salt with *cis*-polar isomer catalyzed by anion column (Scheme 1, reaction 1), whereby a *trans*(O_6) isomer of the $[Ni(1,3\text{-}pddadp)]^{2-}$ is formed. The second way, the most likely one, considers the initial formation of *cis*-polar-$[Ni(1,3\text{-}pddadp)(H_2O)]^-$ with one free 3-propionic arm (Scheme 1, reaction 2). Here 1,3-pddadp ligand plays a role of pentadentate N2O3 ligand and coordinates in same fashion as 1,3-pd2ap [31] producing *cis*-polar isomer so it is easier to understand that after passing through the basic Dowex column (pH > 8) the coordination of remaining six-membered propionic arm and the formation of *trans*(O_6) isomer is most likely to occur.

It is understandable then why the first band contains $[Ni(1,3\text{-}pd2ap)]^-$ and $[Ni(1,3\text{-}pddadp)(H_2O)]^{2-}$ complexes as they are both pentadentates with the same 3D configuration of chelates 1,3-pd2ap and 1,3-pddadp around nickel(II) ion.

In this regard, from all transition metal complexes, which are chelated with the 1.3-pddadp ligand, only the chromium complex gives all three geometric isomers due to *d* electron configuration and specific ionic radii [6,10,11]. In addition, we consider this synthesis as a significant accomplishment were we succeeded in not only preparation but also 3D characterizing the third missing *trans*(O_6) geometric isomer of the $[Ni(1,3\text{-}pddadp)]^{2-}$ complex.

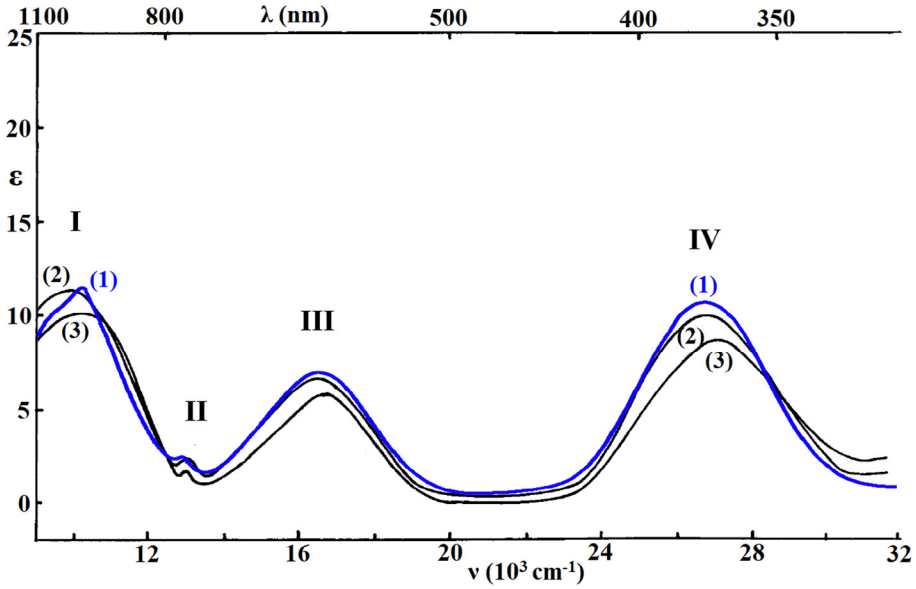

Fig. 4. Electronic absorption spectra of *trans*(O_6)-[Ni(1,3-pddadp)]$^{2-}$ (**1**), *trans*(O_5)-[Ni(1,3-pddadp)]$^{2-}$, (**2**) and *trans*(O_5O_6)-[Ni(1,3-pddadp)]$^{2-}$ (**3**).

Table 6
Absorption data for different isomers of [Ni(1,3-pddadp)]$^{2-}$ complexes.

Complex		Absorption [a]		Assignments	Ref.
		ν_{obs}	ε	O_h	
trans (O_6)-[Ni(1,3-pddadp)]$^{2-}$ (**1**)	I	10.36 (9.55sh)	11.4	$^3A_{2g} \rightarrow {}^3T_{2g}$ (*F*)	This work
	II	13.00	2.9	$\rightarrow {}^1E_g$ (*D*)	
	III	16.64	7.2	$\rightarrow {}^3T_{1g}$ (F)	
	IV	26.81	11.0	$\rightarrow {}^3T_{1g}$ (*P*)	
trans (O_5)-[Ni(1,3-pddadp)]$^{2-}$ (**2**)	I	10.18	11.3		[16]
	II	13.00	2.3		
	III	16.55	6.5		
	IV	26.88	10.0		
trans (O_5O_6)-[Ni(1,3-pddadp)]$^{2-}$ (**3**)	I	10.27	10.0		[16]
	II	13.02	1.8		
	III	16.75	5.7		
	IV	27.17	8.8		

[a] In units of $cm^{-1} \times 10^3$ for the absorption maxima and $dm^3\,mol^{-1}cm^{-1}$ for the molar absorbance (ε).

Table 7
Relative energies (kcal mol^{-1}) for [Ni(1,3-pddadp)]$^{2-}$ isomers.[a]

Method:	Isomer	Energy
B3LYP/TZVP	*trans*(O_5)	1.95
	trans(O_5O_6)	0.42
	trans(O_6)	0.00

[a] The isomer with the lowest energy minimum has been indicated with 0 kcal mol^{-1}.

3.2. Description of the crystal structure of trans(O_6)-[Ba(H_2O)$_4$][Ni(1,3-pddadp)]·4H_2O

A perspective view of the molecular structure of *trans*(O_6)-[Ba(H_2O)$_4$][Ni(1,3-pddadp)]·4H_2O (**1**) complex with the adopted atom-numbering scheme is shown in Fig. 2. Selected metal-ligand bond lengths and bond angles are listed in Table 2. Complex **1** crystallizes in the triclinic crystal system and $P-1$ space group. The asymmetric unit of **1** is built up from binuclear metallic complexes and consists of [Ni(1,3-pddadp)]$^{2-}$ anion and [Ba(H_2O)$_4$(O_G-carbox.)$_2$]$^{2+}$ cation and four water solvent molecules. The Ni1 atom is surrounded by all donating, two N and four O, atoms of the 1,3-pddadp ligand acting in a hexadentate and forming distorted octahedral geometry. The Ba1 atom is coordinated to four water molecules and two bridging carboxylate oxygen atoms, O6 and O7 of the two five-membered glycinate rings (G rings), giving a four-membered ring (Ba1—O6—C6—O7) (Fig. 2).

Two five-membered chelate glycinate rings (G rings) in the complex anion are adopting different conformations, that is, Ni1—N3—C4—C5—O4 ring is in envelope conformation with puckering parameters q_2 = 0.384(3) Å, φ_2 = 37.7(4)° while Ni1—N2—C7—C6—O6 ring adopts half-chair conformation with q_2 = 0.399(3) Å and φ_2 = 19.6(4)° as puckering parameters. The six-membered diamine (T) ring is in twist-boat conformation with puckering parameters: QT = 0.789(3) Å and θ_2 = 89.2(2)°. Two six-membered chelate rings, Ni1—N2—C8—C9—C10—O8 and Ni1—N3—C11—C12—C13—O10, are adopting the same boat conformation where the puckering parameters are: QT = 0.783(3) Å, θ_2 = 86.5(2)° and QT = 0.774(3) Å, θ_2 = 86.4(3)°, respectively.

Both octahedral geometries formed around the central Ni1 and Ba1 atoms are irregular in shape where for [Ni(1,3-pddadp)]$^{2-}$ anion *cis* angles range from 82.12(9)° to 97.26(10)° while the *trans* ones in the complex anion are 175.65(10)°, 174.29(10)° and 171.29 (9)° (Table 2).

The binuclear unit is stabilized by the two coordination bonds, Ba1—O6 (2.784 (2) Å) and Ba1—O7 (2.928 (2) Å), as well as extended hydrogen bonding network (Table 3) involving prevalently the oxygen atoms of the carboxylic groups and the hydrogen atoms of the

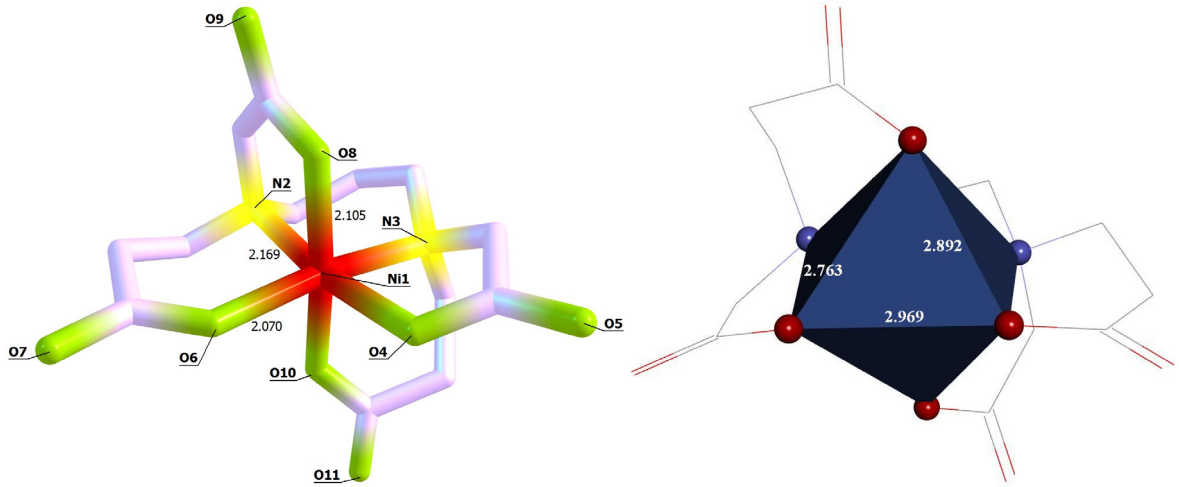

Fig. 5. DFT calculated *trans*(O_5O_6) isomer of $[Ni(1,3\text{-pddadp})]^{2-}$ complex along with irregular shape of octahedron defined by coordinated N2O4 atoms.

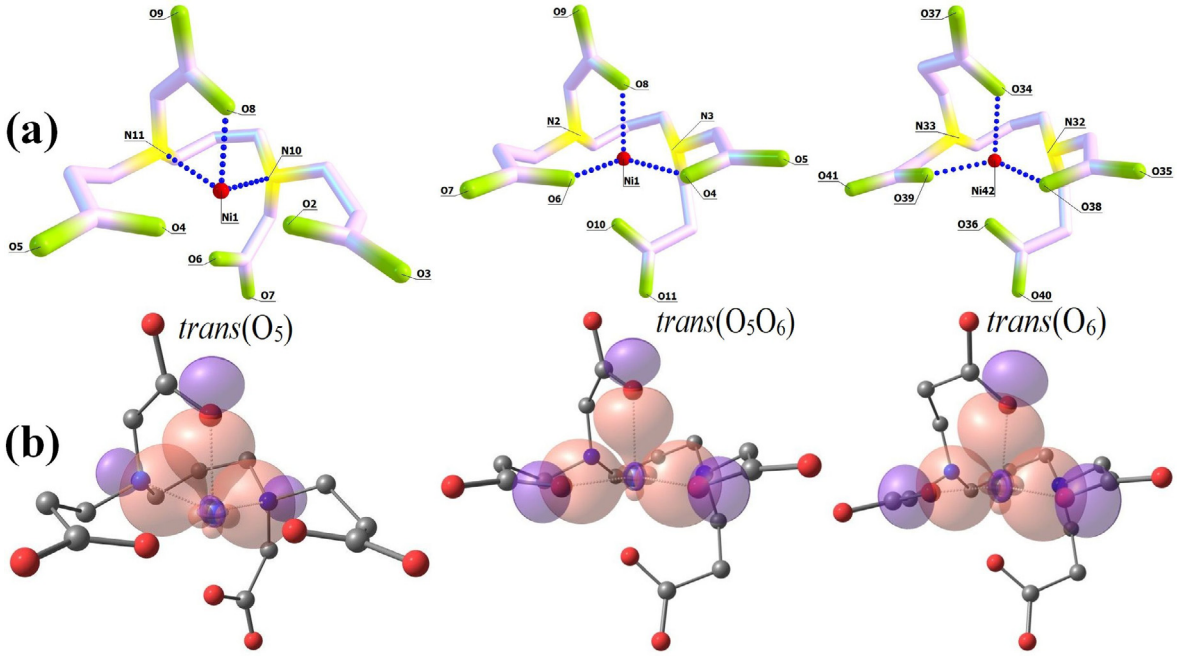

Fig. 6. Structures and bonds (a) and PNBO BD orbitals (b), as a result of NBO analysis on different isomers of $[Ni(1,3\text{-pddadp})]^{2-}$ complex anion (PNBO = pre-orthogonal Natural Bond Orbital).

coordinated and crystal water molecules.

In addition to the dense network of hydrogen bonds present in the crystal packing of **1** (Table 3) Ba1 atom is through four additional coordination bonds, Ba1−O2^2, Ba1−O4^2, Ba1−O5^2 and Ba1−O7^1 (Table 2, Fig. 3), connected to two different binuclear units, which allow the formation of infinite 1-D coordination polymeric chains stretching along *a* axis direction (Fig. 3).

3.3. Strain analysis of $[M(edta\text{-}type)]^{2-}$ complexes in relation to their geometry

Strain analysis of $[M(edta\text{-}type)]^{2-}$ complexes (M = Ni(II), Co(II), Cu(II)) has been performed and discussed in detail. The structural data correlating the stereochemistry of the Ni(II), Co(II) and Cu(II) complexes are given in Table 4. The data are available for complexes *trans*(O_5)-$[Ni(eddadp)]^{2-}$, *trans*(O_5)-$[Ni(1,3\text{-pddadp})]^{2-}$, $[Ni(1,3\text{-pdta})]^{2-}$, *trans*($O_6$)-$[Co(1,3\text{-pddadp})]^{2-}$ and *trans*(O_6)-$[Cu(1,3\text{-pddadp})]^{2-}$, so their parameters are used for comparison [8,16,22,43,44]. For this purpose, the DFT calculated structure was used for complex *trans*(O_5O_6)-$[Ni(1,3\text{-pddadp})]^{2-}$.

The Ni(II), Co(II) and Cu(II) ions adopted octahedral geometry with quite similar degrees of distortion within the complexes. The values of $\Sigma\Delta(O_h)$ parameter are in the range from 39° to 67°. Complex *trans*(O_5)-$Ni(eddadp)^{2-}$ shows the lowest value which is also expected for complexes containing ethylenediamine rings in combination with mixed five/six carboxylate rings [3,4,9]. As expected, the total deviation of the octahedral angles is greatest for a Co(II) complex (67°) and decreasing in a row Co(II) > Ni(II) > Cu(II) with increasing size of the central metal ion (Table 4). Complex *trans*(O_5O_6)-$[Ni(1,3\text{-pddadp})]^{2-}$ (DFT calculated, never 3D determined) with 5-6-6 arrangement of rings shows less distortion (46°) than *trans*(O_6)-$Ni(1,3\text{-pddadp})]^{2-}$ (**1**) and *trans*(O_5)-$Ni(1,3\text{-pddadp})^{2-}$ (the same complexes, but different isomers), so maybe we can expect its crystal structure in the future.

The ethylenediamine (E) ring in the *trans*(O_5)-$Ni(eddadp)^{2-}$ shows a negative value of total deviation, in contrast to the rest of the complexes containing T ring (1,3-propanediamine) which are more relaxed.

Table 8
3-Center, 2-electron A: -Ni-:B hyperbonds (A-Ni:B < = > A:Ni-B) (β electrons).

			NBOs	
Hyperbond A: -Ni-:B	%A-Ni/%Ni-B	occ	BD(A-Ni)	LP(B)
trans(O_5)				
O8:-Ni1-:O6	51.1/48.9	1.9496	55	47
N10:-Ni1-:O4	53.2/46.8	1.9482	56	42
N11:-Ni1-:O2	53.2/46.8	1.9481	57	37
O2:- C12-:O3	52.1/47.9	1.9760	59	40
O4:- C20-:O5	52.1/47.9	1.9758	62	45
trans(O_5O_6)				
O4:-Ni1-:N2	48.0/52.0	1.9328	55	36
O6:-Ni1-:N3	48.6/51.4	1.9365	56	37
O8:-Ni1-:O10	53.0/47.0	1.9616	57	51
O5:- C24-:O4	57.6/42.4	1.9874	66	39
O7:- C25-:O6	56.8/43.2	1.9901	69	43
O11:- C36-:O10	57.5/42.5	1.9825	75	52
trans(O_6)				
O37:- C9-:O34	58.2/41.8	1.9899	85	36
O35:- C10-:O38	57.3/42.7	1.9912	87	45
O40:- C12-:O36	58.1/41.9	1.9885	95	41
O41:- C13-:O39	57.3/42.7	1.9912	98	47
O34:-Ni42-:O36	51.4/48.6	1.9593	99	40
O38:-Ni42-:N33	48.0/52.0	1.9330	100	34
O39:-Ni42-:N32	47.9/52.1	1.9343	101	33

Hyperbonds relating to nickel(II) ion are highlighted in bold.

The five-membered G (in-plane) rings, as supposed, are less than the ideal sum (538.5°), i.e. they are more strained, while six-membered G rings have a positive deviation. The rings in the axial position (R rings) are less strained comparing to G rings due to the presence of a lower number of rings in the environment (Table 4). All complexes show the positive deviation of the M—O—C(R, G) bond angles, except complex *trans*(O_6)-[Cu(1,3-pddadp)]$^{2-}$ in the axial position (−5° for R rings). The total deviation about the N atoms in complex *trans*(O_6)-Ni(1,3-pddadp)]$^{2-}$ (**1**) sum to roughly 12° and this value for other complexes varies from 8° to 14°.

3.4. Spectral analysis

Asymmetric stretching vibrations for Ni-edta type of complexes are given in Table 5. The data are available for similar complexes, so their frequencies are used for comparison. The asymmetric stretching carboxylate frequencies have been established as criteria for distinguishing between protonated carboxylate groups (1700–1750 cm^{-1}) and coordinated carboxylate groups (1560–1680 cm^{-1}) [45–47]. Also, in [M(edta-type)]$^{n-}$ complexes [2,8,12,48], containing the ligands with mixed (five- and six-membered) carboxylate arms, it was clearly demonstrated that the asymmetric stretching frequency of the carboxylate groups of the five-membered rings lies at higher energy (ca. 1600–1680 cm^{-1}) [49] than the corresponding frequency of the six-membered chelate rings (ca. 1560–1600 cm^{-1}) [49]. In addition, the carboxylate spectral region was found to be useful for distinguishing geometrical isomers in these types of complexes [2,8,12,48]. It is known that C_2 symmetry complexes (*trans*(O_5) and *trans*(O_6)) exhibit two intensive bands corresponding to the rings in-plane and axial position, while non-symmetric C_1 symmetry complexes (*trans*(O_5O_6) show four intensive bands that are in accordance to the four non-equivalent carboxyl groups.

In the expected IR carboxylate region, the complex shows absorption in agreement with its C_2 molecular symmetry. Normally, one strong band centered at 1598 cm^{-1} and one shoulder at 1575 cm^{-1} are observed due to the asymmetric vibrations of five-membered acetate rings and six-membered 3-propionate rings, respectively (Fig. S1, ESI). The lack of other absorptions in the 1700–1750 cm^{-1} range in the spectra of this complex suggests that all the carboxylate groups are coordinated.

The ligand field absorption spectra for different geometrical isomers of Ni(1,3-pddadp)$^{2-}$ complex are given in Fig. 4 (Table 6). The six-membered diamine (T) rings, due to the influence of tetragonality on the spectrochemical behavior of these complexes (D_{4h} model), show broadening of lower energy side of the first absorption band. This is particularly important when *trans*(O_6) isomer is in question. The first band shows an obvious splitting due to D_{4h} tetragonality (the difference between $(Ni\text{-}O)_{axial}$ = 2.129 and $(Ni\text{-}O)_{equatorial}$ = 2.038 Å bonds is an apparent example). However, its electronic absorption spectra, as established for the Ni(II)-edta-type and most other Ni(II) complexes, can best be interpreted by using an octahedral model (O_h): $^3A_{2g} \rightarrow {}^3T_{2g}(F)$ (band I); $^3A_{2g} \rightarrow {}^3T_{1g}(F)$ (band III) and $^3A_{2g} \rightarrow {}^3T_{1g}(P)$ (band IV) (Table 6). As expected, the aqueous spectra of all geometric isomers show a shoulder at approximately 13,000 cm^{-1} which occurs on the high-energy side of the first spin-allowed band (band II, Table 6). This band probably arises from a spin-forbidden triplet to singlet transition. The absorption maxima position of the first and third band are usually used for comparison of average ligand field strength (LFS). LFS for these complexes (Table 6) increases in the order *trans*(O_5) < *trans*(O_5O_6) ≤ *trans*(O_6) with the decreasing number of six-membered rings in the G plane.

3.5. Computational chemistry

3.5.1. DFT calculations

We have used G09 quantum-mechanical code for the study of Ni(II) complexes. The potential geometric isomers were optimized using heavy Ahlrich's TZVP basis set. Table 7 contains the energy order of different geometric isomers of [Ni(1,3-pddadp)]$^{2-}$ complexes. Recently, we reported the inability of ADF2017.1 (PW91/TZ2P+) [50] to optimize *trans*(O_6) isomer. This could be a consequence of the wrong initial coordinates or choice of generalized gradient approximation (GGA) form/basis set [31]. For all complexes, the DFT theory (B3LYP/TZVP) gave the lowest energy for the isomer in question (Table 7). Quantum mechanical calculation shows that *trans*(O_6) isomer is 0.53 kcal mol^{-1} more stable than *trans*(O_5O_6) and 1.95 kcal mol^{-1} more stable than *trans*(O_5) (Table 7). Apparently that almost all bonds are slightly longer (Fig. 5) than ones found in crystal structures. This might be attributed to the DFT calculations on molecules implicited by the water as a dielectric but also to the choice of DFT method and basis set.

3.5.2. Natural bonding orbital analysis (NBO)

We used GENNBO 6.0 to analyze Gaussian output 0.47 files. 3D structures of different isomers are depicted in Fig. 6. NBO search for the best Lewis structure, calculated from 0.47 files, gave one molecular [Ni(1,3-pddadp)]$^{2-}$ unit in case of all the isomers. In general, according to NBO analysis, all the isomers represent strongly delocalized structures.

NBO search for the best Lewis structure solution, in case of all isomers, found that molecular units in the alpha (α) and beta (β) systems are inequivalent. The domination of donor/acceptor interactions naturally arises from the β spin system, which retains unfilled s or d population throughout the series [51]. Therefore, for labeling purposes, the molecular units of the β system will be used here. Generally, all the isomers give roughly 99.1% of Lewis (L) occupancies and 1.7% of valence non-Lewis (NL) orbitals (Table 8). The rest of ~0.2% occupancies belong to Rydberg and Core orbitals. There are three Ni—N(O) bonds which are described with three L bonding (BD) orbitals (Fig. 6) followed by three high-energy valence NL antibonding (BD*) orbitals. Further, NBO search found three 3-center 2-electrons (β system) A:-Ni-:B (A,B = N_{amine} or $O_{carboxylate}$) hyperbonds (ω bonds) along with O:-C-:O carboxylate triads. These 3-center metal bonds, constituting of A(N_{amine} or $O_{carboxylate}$), Ni and B(N_{amine} or $O_{carboxylate}$) atoms, with strongly interacting valence hybrids h_A, h_{Ni}, h_B, are described as a strong resonance hybrid of the two localized L structure

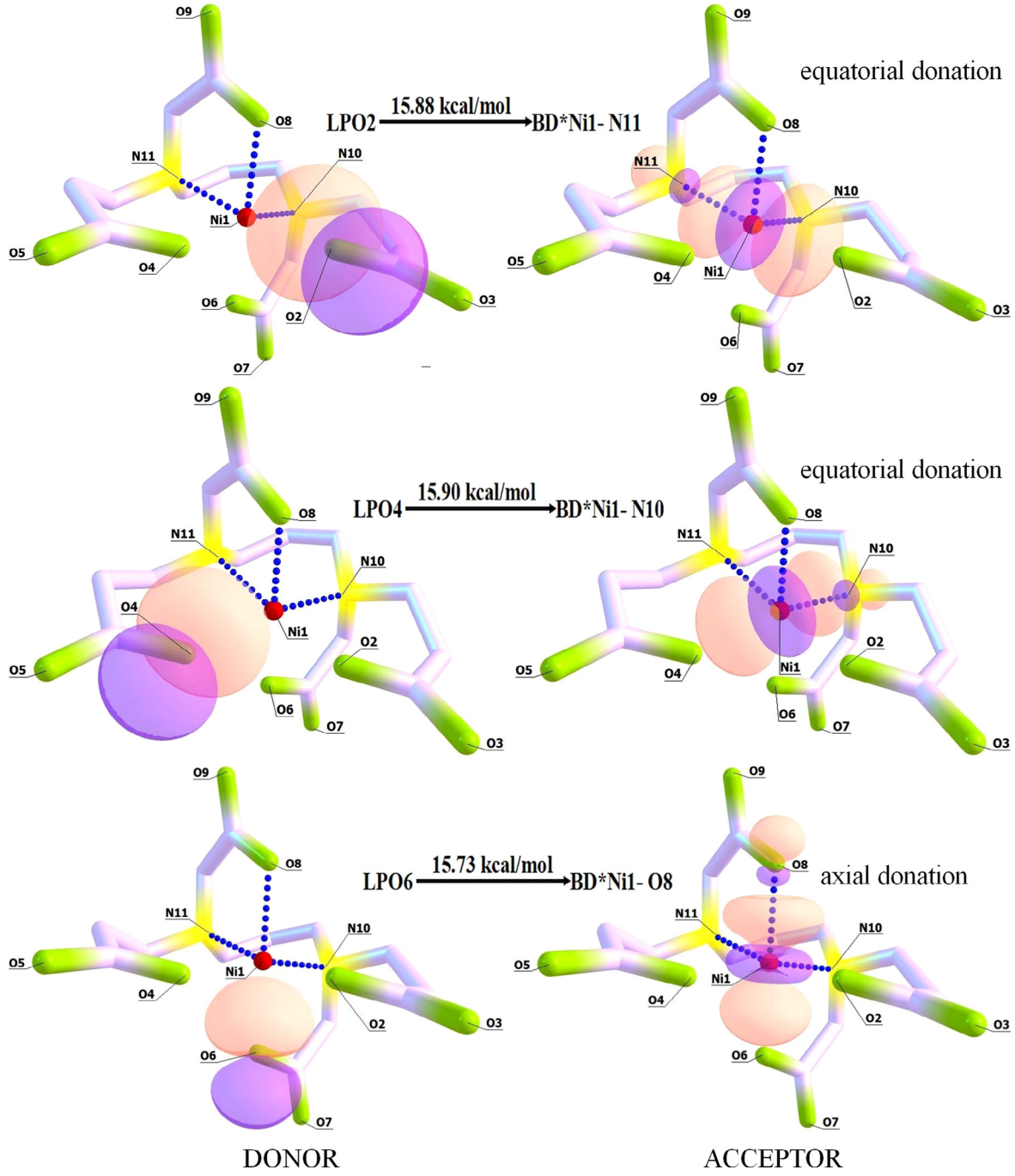

Fig. 7. Donor to Acceptor charge transfer referred to as resonance hybrid stabilization of *trans*(O_5)-[Ni(1,3-pddadp)]$^{2-}$ complex anion.

representations:

A− Ni: B↔ A: Ni − B (A, B= N_{amine} or $O_{carboxylate}$)

These triad resonances account on interactions between LP $n_{B(A)}$ and BD $\sigma_{NiA(B)}$ orbitals.

Strictly speaking, using NBO language, each A: -Ni-:B triad corresponds to strong $n_B \rightarrow \sigma_{NiA*}$ delocalization in the A-Ni:B Lewis structure, or equivalently, strong $n_A \rightarrow \sigma_{NiB*}$ delocalization in the alternative A: Ni-B Lewis structure, leading to nearly equivalent NRT weightings of these structures ($w_{A\text{-}Ni:B} \approx w_{A:\ Ni\text{-}B}$) [51]. The BD* (valence shell NL orbitals) typically play the primary role in departures (delocalization) from the idealized Lewis structure. The second-order perturbative estimates, donor(D)-acceptor(A) (bond-antibond) theory analysis of Fock matrix, interactions in the NBO basis. This is carried out by examining all possible interactions between "filled" (donor, L) NBOs and "unfilled" (acceptor, NL) NBOs, and estimating their energetic importance by 2nd-order perturbation theory. These interactions are referred to as "delocalization" corrections to the zeroth-order natural Lewis structure [51]. We already mentioned above that molecular stabilization comes from delocalization caused by $n_A \rightarrow \sigma_{NiB*}$ or $n_B \rightarrow \sigma_{NiA*}$ charge transfer. NBO really found three high-energy valence NL BD* orbitals, containing nickel, for each isomer structure. In the case of *trans*(O_5) isomer, these valence NL BD* orbitals are: 102. (0.08026) BD* Ni1-O8, 103. (0.08186) BD* Ni1-N10 and 104. (0.08179) BD* Ni1-N11 (Fig. 7 – Acceptor). One may see (numbers in parentheses) significantly large NL occupation (roughly 0.08 electrons) for each antibonding orbital. Each of these orbitals receive a donation of electron density from, symmetry-related, Lewis non-bonding lone pairs (LP), sp^n orbitals. These LP

orbitals are depicted in Fig. 7. (Donor): $sp^{6.58}$ (O2), $sp^{6.58}$ (O4) and sp^{13} (O_6). Therefore, according to D/A mechanism we are estimating three principal electron density transfers given in Fig. 7. Under the term "principal electron density transfer" we mean only those transfers where the LP orbital directionality does not deviate much from corresponding BD* orbital line. Of course, in such strongly delocalized structures, there appears delocalization that comes from donor LP orbitals of different orientations as well. However, such a D/A transfers are less important and energy poorer than those listed and do not significantly contribute to the stabilization of the resonant hybrid. Thus, making a comparison between energies that come from principal electron density transfers of different isomers the next order has been established:

$$trans(O_5)\text{: }trans(O_6)\text{: }trans(O_5O_6) = 47.56\text{: }42.37\text{: }40.93\ kcal\ mol^{-1}$$

Such an energy relationship tells us that the stabilization of the hybrid structure is greatest in the case of the *trans*(O_5) isomer and amounts more than 5 kcal mol^{-1}. This could be a rational explanation of why the *trans*(O_5) isomer is favorable compared to other isomers despite the established order of their electronic energies (Table 7).

4. Conclusions

We report synthesis and characterization of hexadentate nickel(II) complex *trans*(O_6)-[Ba(H_2O)$_4$][Ni(1,3-pddadp)]·4H_2O containing symmetrical edta-type 1,3-pddadp^{4-} ligand. In this isomer, the two five-membered acetate rings along with two nitrogen (G rings) lie in the equatorial plane while the two 3-propionate rings occupy axial line (R rings). The structural assignment was made based on the DFT, IR and UV–Vis spectral data analysis. Spectral IR and UV–Vis data indicate octahedral coordination around nickel with all carboxylate groups being coordinated/deprotonated. Extensive strain analysis of [M(edta-type)]$^{2-}$ complexes (M = Ni, Co, Cu) in combination with results of DFT investigations revealed that 3D structure of *trans*(O_5O_6)-[Ni(1,3-pddadp)]$^{2-}$ is quite stable with a minimum strain. Generally, DFT theory shows that *trans*(O_6) isomer is 0.53 kcal mol^{-1} more stable than *trans*(O_5O_6) and 1.95 kcal mol^{-1} more stable than *trans*(O_5). Provided DFT/NBO analysis (β-electrons) suggest that within all of the investigated isomers of Ni(l,3-pddadp)$^{2-}$ anion there is one distinct ionic unit of nickel(II)-edta-type. The unit exhibits a strong Donor-Acceptor mechanism. Also, NBO analysis for all three isomers predicts the existence of a 3-center 2-electron (β system) A: -Ni-: B hyperbonds along with O:-C-:O carboxylate triads. The Second-Order Perturbation Theory Analysis predicts molecular stabilization that comes from delocalization caused by $n_A \rightarrow \sigma_{NiB^*}$ or $n_B \rightarrow \sigma_{NiA^*}$ charge transfer. By comparing the energies originating from principal electron density transfers of different isomers, the following order was determined: *trans*(O_5):*trans*(O_6):*trans*(O_5O_6) = 47.51:42.37:40.93 kcal mol^{-1}, which tells us that the stabilization of the hybrid structure is greatest in the case of the *trans*(O_5) isomer (> 5 kcal mol^{-1}). The obtained result can explain why the *trans*(O_5) isomer is favorable despite the order that was established by DFT calculated electronic energies.

Acknowledgements

The authors gratefully acknowledge financial support from the Ministry of Education, Science and Technological Development of the Republic of Serbia (Projects No. III41010 and 172057).

Appendix A. Supplementary data

Supplementary data to this article can be found online at https://doi.org/10.1016/j.ica.2019.118954.

References

[1] D.J. Radanović, Coord. Chem. Rev. 54 (1984) 159–261 (and references therein).
[2] D.J. Radanović, B.E. Douglas, J. Coord. Chem. 4 (1975) 191–198.
[3] T. Mizuta, T. Yamamoto, N. Shibata, K. Miyoshi, Inorg. Chim. Acta 169 (1990) 257–263.
[4] R. Herak, Lj. Manojlović-Muir, M.I. Djuran, D.J. Radanović, J. Chem. Soc., Dalton Trans. (1985) 861–864.
[5] F.T. Helm, W.H. Watson, D.J. Radanović, B.E. Douglas, Inorg. Chem. 16 (1977) 2351–2354.
[6] T. Yamamoto, K. Mikata, K. Miyoshi, H. Yoneda, Inorg. Chim. Acta 150 (1988) 237–244.
[7] K. Kanamori, J. Kumada, M. Yamamoto, T. Okayasu, K. Okamoto, Bull. Chem. Soc. Jpn. 68 (1995) 3445–3451.
[8] D.J. Radanović, S. Ianelli, G. Pelosi, Z.D. Matović, S. Tasicć-Stojanović, B.E. Douglas, Inorg. Chim. Acta 278 (1998) 66–75.
[9] M. Parvez, C. Maricondi, D.J. Radanović, M.I. Djuran, B.E. Douglas, Inorg. Chim. Acta 182 (1991) 177–186.
[10] B.E. Douglas, D.J. Radanović, Coord. Chem. Rev. 128 (1993) 139–165 (and references therein).
[11] S. Kaizaki, M. Byakuno, M. Hayashi, J.I. Legg, K. Umakoshi, S. Ooi, Inorg. Chem. 26 (1987) 2395–2399.
[12] D.J. Radanović, B.V. Prelesnik, D.D. Radanović, Z.D. Matović, B.E. Douglas, Inorg. Chim. Acta 262 (1997) 203–211.
[13] D.J. Radanović, S.R. Trifunović, M.S. Cvijović, C. Maricondi, B.E. Douglas, Inorg. Chim. Acta 196 (1992) 161–169.
[14] M. Parvez, C. Maricondi, D.J. Radanović, S.R. Trifunović, V.D. Miletić, B.E. Douglas, Inorg. Chim. Acta 248 (1996) 89–92.
[15] U. Rychlewska, M.I. Djuran, M.M. Vasojević, D.D. Radanović, V.M. Ristanović, D.J. Radanović, Inorg. Chim. Acta 328 (2002) 218–228.
[16] Z.D. Matović, S. Ianelli, G. Pelosi, S.K. Janićijević, V.M. Ristanović, G. Ponticelli, D.J. Radanović, Polyhedron 21 (2002) 2667–2674.
[17] H.A. Weakliem, J.L. Hoard, J. Am. Chem. Soc. 81 (1959) 549–555.
[18] E.F.K. McCandlish, T.K. Michael, J.A. Neal, E.C. Lingafelter, N.J. Rose, Inorg. Chem. 17 (1978) 1383–1394 (and references therein).
[19] E. Coronado, M. Drillon, A. Fuertes, D. Beltran, A. Mosset, J. Galy, J. Am. Chem. Soc. 108 (1986) 900–905.
[20] J.M. Nesterova, M.A. Porai-Koshits, Koord. Khim. 10 (1984) 129.
[21] M.V. Leont'eva, A.Ya. Fridman, N.M. Dyatlova, V.M. Agre, T.F. Sysoeva, Z. Neorg. Khim. 32 (1987) 2494.
[22] D.J. Radanović, T. Ama, H. Kawaguchi, N.S. Drašković, D.M. Ristanović, S. Janićijević, Bull. Chem. Soc. Jpn. 74 (2001) 701–706 (and references therein).
[23] D.J. Radanović, V.D. Miletić, T. Ama, H. Kawaguchi, Bull. Chem. Soc. Jpn. 71 (1998) 1605–1614.
[24] D.J. Radanović, N. Sakagami, V.M. Ristanović, S. Kaizaki, Inorg. Chim. Acta 292 (1999) 16–27.
[25] R.H. Nuttall, D.M. Stalker, Talanta 24 (1977) 355–360.
[26] J.J. Stezowski, R. Countryman, J.L. Hoard, Inorg. Chem. 12 (1973) 1749–1754.
[27] J.P. Fackler Jr., F.J. Kristine, A.M. Mazany, T.J. Moyer, R.E. Shepherd, Inorg. Chem. 24 (1985) 1857–1860.
[28] M.S. Jeremić, M.D. Radovanović, F. Bisceglie, V.V. Kojić, R. Jelić, Z.D. Matović, Polyhedron 156 (2018) 19–30.
[29] E.D. Glendening, C.R. Landis, F. Weinhold, J. Comput. Chem. 34 (2013) 1429–1437.
[30] K. Igi, B.E. Douglas, lnorg. Chem. 13 (1974) 425–430.
[31] S. Belošević, M. Čendić, M. Djukić, M. Vasojević, A. Meetsma, Z.D. Matovic, Inorg. Chim. Acta 399 (2013) 146–153.
[32] Oxford Diffraction CrysAlis CCD and CrysAlis Red. Oxford Diffraction, (2009).
[33] P. Coppens, F.R. Ahmed, S.R. Hall, C.P. Huber (Eds.), Crystallographic Computing, Munksgaard, Copenhagen, 1970, pp. 255–270.
[34] G.M. Sheldrick, Crystal structure refinement with SHELXL, Acta Crystallogr., Sect. C: Struct. Chem. 71 (2015) 3–8.
[35] A.L. Spek, J. Appl. Crystallogr. 36 (2003) 7–13.
[36] L.J. Farrugia, WinGX suite for small-molecule single-crystal crystallography, J. Appl. Crystallogr. 32 (1999) 837–838.
[37] C.F. Macrae, I.J. Bruno, J.A. Chisholm, P.R. Edgington, P. McCabe, E. Pidcock, L. Rodriguez-Monge, R. Taylor, J. van de Streek, P.A. Wood, J. Appl. Cryst. 41 (2008) 466–470.
[38] M.J. Frisch, G.W. Trucks, H.B. Schlegel, G.E. Scuseria, M.A. Robb, J.R. Cheeseman, G. Scalmani, V. Barone, B. Mennucci, G.A. Petersson, H. Nakatsuji, M. Caricato, X. Li, H.P. Hratchian, A.F. Izmaylov, J. Bloino, G. Zheng, J.L. Sonnenberg, M. Hada, M. Ehara, K. Toyota, R. Fukuda, J. Hasegawa, M. Ishida, T. Nakajima, Y. Honda, O. Kitao, H. Nakai, T. Vreven, J.A. Montgomery Jr., J.E. Peralta, F. Ogliaro, M. Bearmark, J.J. Heyd, E. Brothers, K.N. Kudin, V.N. Staroverov, R. Kobayashi, J. Normand, K. Raghavachari, A. Rendell, J.C. Burant, S.S. Iyengar, J. Tomasi, M. Cossi, N. Rega, J.M. Millam, M. Klene, J.E. Knox, J.B. Cross, V. Bakken, C. Adamo, J. Jaramillo, R. Gomperts, R.E. Stratmann, O. Yazyev, A.J. Austin, R. Cammi, C. Pomelli, J.W. Ochterski, R.L. Martin, K. Morokuma, V.G. Zakrzewski, G.A. Voth, P. Salvador, J.J. Dannenberg, S. Dapprich, A.D. Daniels, O. Farkas, J.B. Foresman, J.V. Ortiz, J. Cioslowski, D.J. Fox, Gaussian 09, Revision D.01, Gaussian, Inc., Wallingford CT, 2013.
[39] MOPAC2016, J.J.P. Stewart, Stewart Computational Chemistry, Colorado Springs, CO, USA, HTTP://OpenMOPAC.net (2016).
[40] (a) A.D. Becke, J. Chem. Phys. 98 (1993) 5648–5652;
(b) C. Lee, W. Yang, R.G. Parr, Phys. Rev. B 37 (1988) 785–789;

(c) B. Miehlich, A. Savin, H. Stoll, H. Preuss, Chem. Phys. Lett. 157 (1989) 200–206.
[41] F. Weigend, R. Ahlrichs, Phys. Chem. Chem. Phys. 7 (2005) 3297–3305.
[42] E.D. Glendening, J. Phys. Chem. A 109 (2005) (1940) 11936–11941.
[43] S. Grubišić, D.D. Radanović, U. Rychlewska, B. Warzajtis, N.S. Drašković, M.I. Djuran, S.R. Niketić, Polyhedron 26 (2007) 3437–3447.
[44] M. Ćendić, R.J. Deeth, A. Meetsma, E. Garribba, D. Sanna, Z.D. Matović, Polyhedron 124 (2017) 215–228.
[45] D.H. Busch, J.C. Bailar Jr., J. Am. Chem. Soc. 75 (1953) 4574–4575.
[46] M.L. Morris, D.H. Busch, J. Am. Chem. Soc. 78 (1956) 5178–5181.
[47] K. Nakamoto, Infrared Spectra of Inorganic and Coordination Compounds, Wiley, New York, NY, 1963.
[48] a) K.D. Gailey, D.J. Radanović, M.I. Djuran, B.E. Douglas, J. Coord. Chem. 8 (1978) 161–167;
b) J.A. Neal, N.J. Rose, Inorg. Chem. 7 (1968) 2405–2412;
c) J.A. Neal, N.J. Rose, Inorg. Chem. 12 (1973) 1226–1232.
[49] a) K. Nakamoto, Y. Morimoto, A.E. Martell, J. Am. Chem. Soc. 83 (1961) 4528–4532;
b) M.B. Ćelap, S.R. Niketić, T.J. Janjić, V. Nikolić, Inorg. Chem. 6 (1967) 2063–2065.
[50] S. Belošević, M.M. Vasojević, M.S. Jeremić, A. Meetsma, Z.D. Matović, J. Coord. Chem. 66 (2013) 1730–1745.
[51] F. Weinhold, C.R. Landis, Valency and Bonding: A Natural Bond Orbital Donor-Acceptor Perspective, Cambridge University Press, 2005.